

# TSUNAMI3D Benchmark Results for 2017 NTHMP Tsunamigenic Landslide Model Benchmarking Workshop

Wei Cheng, Juan Horrillo, Richards C. Sunny \*

July 2017

## Abstract

Recent works by various tsunami modelers have shown that landslide tsunami hazard may be dominant along significant parts of the US coastline, as compared to hazards from other tsunamigenic sources. To understand numerical model's capability in reproducing this phenomenon, the National Tsunami Hazard Mitigation Program (NTHMP) has indicated that all numerical tsunami models used for mapping products should be validated and compared through a model benchmarking workshop/process to determine their accuracy and consistency between other model's methods. Consequently, a workshop was held on January 9-11, 2017 in Texas A&M University at Galveston where seven different benchmark cases were stated for the workshop, among which three were required to be reproduced for all participants. This paper discusses the results of the three required benchmark problems by the TSUNAMI3D model. Benchmark problems were designed to validate model's capability to reproduce the wave generation stage, propagation and runup for 2D and 3D submarine landslides, also aimed to visualize the importance of physical versus numerical dissipation and the variability of results between different model's approaches. The numerical model TSUNAMI3D is a fully 3D Navier-Stokes (NS) model optimized for tsunami problems. The model solves transient fluid flow with free surface boundaries based on the volume

---

\*Texas A&M University at Galveston

of fluid (VOF) method. For each benchmark problem, we use first or second order accuracy for nonlinear terms and bottom/wall friction formulation based on the logarithmic law of the wall. In general, for large scale scenarios (massive landslide), the landslide material is model as a Newtonian flow. Also, the landslide granular material can be regarded as a dense fluid with frictional internal rheology. Overall, for all problems, this model produces results in good agreement with the experimental and observational data, matching expected magnitudes and periodicity.

Validation works confirm that 3D models with simplified landslide mechanism can then be used to understand and reproduce the complex wave propagation patterns and wave runups generated by landslides. We hope that application of the numerical models presented here can help assessing tsunami hazards for communities located in proximity of potential landslide hazards. Also, the set of benchmark problems can be used for further numerical model validations, helping tsunami organizations, e.g., the NTHMP, to develop approaches and tune up its numerical models to makes decisions that would save lives and property.

## 1 Model Background

TSUNAMI3D is a 3D Navier-Stokes (NS) model which is optimized for tsunami problems and is based on the computational fluid dynamics (CFD) model originally developed at Los Alamos National Laboratory (LANL) during the 1970s, following early work by Hirt and Nichols (1981). It solves transient fluid flow with free surface boundaries based on the concept of the fractional volume of fluid (VOF) method using an Eulerian mesh of rectangular cells of variable size in all directions. The fluid equations solved are the finite difference approximation of the full NS equations in Cartesian coordinates and the incompressibility condition equation which results from the continuity equation when the density is constant. The basic mode of operation is for a single fluid phase having multiple free surfaces. However, TSUNAMI3D also can be used for calculations involving two fluid phases separated by a sharp or diffusive interface, for instance, water and landslide material. In either case, both fluids are considered incompressible and treated as Newtonian. Also, landslide material can be regarded as a dense fluid with frictional internal rheology. Internal obstacles, e.g., topography, walls, etc.,

are defined by blocking out, fully or partially, any desired combination of cells in the domain. TSUNAMI3D has led to very good agreement (Horrillo et al., 2013) with the standard provided by the National Tsunami Hazard Mitigation Program (NTHMP) for validation and verification of tsunami model inundation, report OAR-PMEL-135 (Synolakis et al., 2007). Results from validation and verification of the model can be also found in the NTHMP’s Workshop Proceedings (NTHMP 2012) and Horrillo, et al. (2014). The interested reader is referred to Horrillo (2006) and Horrillo et al. (2013) for more detailed information about the 3D NS model.

## 2 Description of the Numerical Models

In TSUNAMI3D the governing equations to describe the flow of two incompressible Newtonian fluids (*e.g.*, water and landslide) is indicated below,

$$\frac{\partial u_i}{\partial x_i} = 0, \quad i = 1, 2, 3 \quad (1)$$

and the nonconservative equation of momentum given by:

$$\begin{aligned} \frac{\partial u_i}{\partial t} + u_j \frac{\partial u_i}{\partial x_j} = & -\frac{1}{\rho_{1,2}} \left( \frac{\partial p}{\partial x_i} + \frac{\partial q}{\partial x_i} \right) \\ & + \frac{\partial}{\partial x_j} \left[ \frac{\mu_{1,2}}{\rho_{1,2}} \left( \frac{\partial u_i}{\partial x_j} + \frac{\partial u_j}{\partial x_i} \right) \right] + g_i, + F_{r_2} \quad (2) \\ & i, j = 1, 2, 3 \end{aligned}$$

where  $\mathbf{u} = [u(x, y, z, t), v(x, y, z, t), w(x, y, z, t)]$  are the velocity components along the coordinate axes  $[x, y, z]$  at time  $t$ . Here, the given subscripts 1, 2 indicate physical variables corresponding to the water and landslide phases, i.e.,  $\rho_1(x, y, z, t)$  and  $\rho_2(x, y, z, t)$  are the density of the water and landslide material, respectively. The water and landslide phases are considered as Newtonian fluids, therefore the kinematic viscosity  $\nu_1 = \mu_1/\rho_1$  and  $\nu_2 = \mu_2/\rho_2$  can be adjusted for internal friction. Here  $\mu_1$  and  $\mu_2$  are the molecular viscosity of the water and landslide material respectively, thus, the landslide friction term in Eq. 2 factored by  $\mu_2/\rho_2$  can be also changed according to a constitutive model for landslide rheology, *e.g.*, the Bingham model; however this method was not implemented in this study and, instead,

we adopted a more simplistic friction term,  $F_{r_2}$ , which is discussed later on. The acceleration due to gravity is represented by  $\mathbf{g} = [0, 0, -g]$ . The total pressure in each phase,  $P_{tot} = p + q$ , is divided into the hydrostatic pressure  $p$  and the dynamic or non-hydrostatic pressure  $q$ .

In the water domain, the hydrostatic pressure is given by:

$$p = \rho_1 g (\eta_1 - z) \quad (3)$$

such that  $\partial p / \partial z = -\rho_1 g$ . Here,  $z$  is the elevation measured from the vertical datum to the cell center and  $\eta_1$  is the water free surface elevation, also measured from the vertical datum. For the landslide phase, the total pressure  $P_{tot} = p + q$ , is determined by the hydrostatic pressure as:

$$p = g[\rho_1(\eta_1 - \eta_2) + \rho_2(\eta_2 - z)] \quad (4)$$

and the dynamic pressure  $q$ . Here  $\eta_2$  is the landslide free surface elevation measured from the vertical datum. The landslide material is usually modeled as a Newtonian fluid, with kinematic viscosity,  $\nu_2 = \mu_2 / \rho_2$  for internal friction. To bring the Newtonian fluid to a stop (i.e., mimicking a non-Newtonian flow), an additional term in the momentum equation is included, by regarding the mass of the landslide material as a dense fluid (no change of volume) with a purely frictional internal rheology. Thus, a Coulomb type friction force  $F_{r_2}$ , [Heinrich and Piatanesi, 2000] is added to mimic the granular flow behavior, given by

$$F_{r_2} = g(1 - \rho_1 / \rho_2) \cos(\theta) \tan(\phi_{1,2}) u / |u| \quad (5)$$

The internal friction force always acts in the opposite direction of the velocity vector  $\mathbf{u}$ , which is achieved by the term  $u / |u|$ . The parameter  $\theta$  is the local bottom slope with respect to  $x - y$  axes plane. Parameters  $\tan(\phi_1)$  and  $\tan(\phi_2)$  are the Coulomb type landslide internal friction and the basal friction coefficients, respectively. The parameter  $\tan(\phi_1)$  is given to any internal or embedded landslide material parcel, i.e., a landslide cell surrounded by landslide cells. Likewise, parameter  $\tan(\phi_2)$  accounts for the friction coefficient of landslide parcel in contact with the material of the sea bottom (slope failure plane) or experimental basin bottom.

The internal friction coefficient  $\tan(\phi_1)$  is calculated by following a simple constitutive friction law or empirical shape function  $\varphi(I)$ , [Forterre and Pouliquen, 2008] for immersed granular material under a viscous regime.

$$\tan(\phi_1) = \varphi(I) = \varphi_s + \frac{\varphi_2 - \varphi_s}{I_o / I + 1} \quad (6)$$

where  $I = |\dot{\gamma}| \mu_{eff} / P_{tot}$ , is a dimensionless parameter called the inertia number, and  $\dot{\gamma}_{ij} = \partial u_i / \partial x_j + \partial u_j / \partial x_i$  is the strain rate tensor.  $|\dot{\gamma}| = (0.5 \dot{\gamma}_{ij} \dot{\gamma}_{ij})^{0.5}$  is the second invariant of  $\dot{\gamma}_{ij}$ . In this rheology,  $\mu_{eff}$  is an effective viscosity and  $P_{tot}$  is the confined pressure. The shape function  $\varphi(I)$ , Eq. 6, starts from a critical or minimum friction coefficient value of  $\varphi_s = \tan(\phi_s)$  at zero shear rate or low  $I$  and converges to a limiting value of  $\varphi_2 = \tan(\phi_2)$  at high  $I$ . Here  $I_o$  is a constant value obtained through physical experiments or by means of a back-analysis from numerical results.

In general, 3D Numerical results are very sensitive to space and time step resolutions and require substantial computational time and resources; therefore, the selected time step requires to be adjusted in order to optimize performance under the stability constraints, such as the advection and diffusion conditions. For this reason, the 3D model tested here, TSUNAMI3D, has been optimized to reduce the computational burden by using the standard VOF algorithm and the donor-acceptor technique, described by [Hirt and Nichols, 1981]. In addition, the pressure term is split into hydrostatic and non-hydrostatic, achieving faster convergence (in most cases) for the solution of Poisson equation. The interested reader is referred to [Horrillo, 2006] and [Horrillo et al., 2013] for more detailed information.

### 3 Numerical solution Method

The fluid equations are solved using standard finite difference schemes. All variables are treated explicitly except for the non-hydrostatic pressure  $q$  which is solved implicitly. The nonlinear terms in the momentum equations are solved using a first order upwind scheme or, alternatively, a second order conservative scheme which includes a flux limiter to maintain monotonicity of the velocities. Artificial viscosity in the model arises mainly from the truncation error of the scheme used for the nonlinear terms. The non-hydrostatic pressure  $q$  is calculated through the pressure Poisson equation by using the incomplete Cholesky conjugate gradient method to solve the resulting linear system of equations.

The free surface elevation  $\eta$  is traced using the simplified VOF method based on the scalar function and the donor-acceptor algorithm of [Hirt and Nichols, 1981]. The method is based on the so-called fraction function  $F$ , in which  $F$  is defined as the fraction of fluid in the control volume cell (namely, volume of a computational grid cell).  $F$  is a discontinuous function, its value varying

from 0 to 1 depending on the fluid interface location. That is, when the cell is empty, the cell has no fluid inside and the value of  $F$  is zero; in contrast, when the cell is full,  $F = 1$ . When the fluid's interface is within the cell,  $0 < F < 1$ , which defines the location of the free surface. Integration of individual cell fluxes determines the change in  $F$  within a cell, and thus, the change in sea level and landslide-water interface.

## 4 Benchmark Problem Comparisons

### 4.1 Benchmark Problem #2 - Three-dimensional submarine solid block

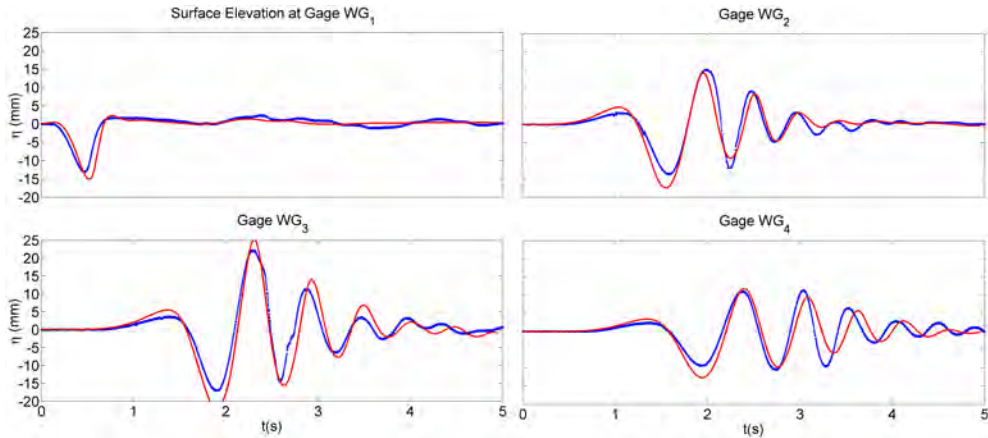


Figure 1: Comparison of gauge time series between TSUNAMI3D (red) and 3D solid block landslide experiment (blue) (case  $d=61$  mm).

The computational domain used in TSUNAMI3D for both  $d = 61$  mm and  $d = 120$  mm cases is 5.0 m by 2.2 m by 1.36 m in the  $x$ ,  $y$ , and  $z$  directions, respectively. Cell sizes are 10 mm in both  $x$  and  $y$  directions and  $\sim 2.7$  mm in  $z$ . This results in 55.9 million computational cells. The simulation ran for 5 s at a time step  $\Delta t$  of 0.001 s. Radiation boundary conditions are applied to all walls except for the runup side. No-slip boundary condition is applied to the bottom, and eddy viscosity for the water has been set to  $1 \times 10^{-6}$  m<sup>2</sup>/s. The 3D solid slide motion is prescribed according to the experiment

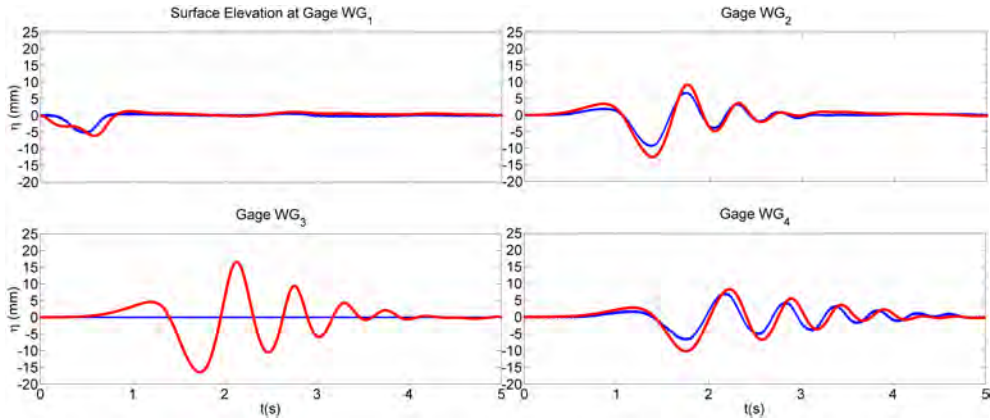


Figure 2: Comparison of gauge time series between TSUNAMI3D (red) and 3D solid block landslide experiment (blue) (case  $d=120$  mm).

measurement, which is achieved by a moving bottom profile and velocity boundary condition.

Fig. 1 and Fig. 2 show well matching wave period and magnitude between experiment (blue) and simulation result (red). The trailing waves from TSUNAMI3D travel slightly slower than the experiment and wave magnitudes are slightly bigger for the first few waves. Nonetheless, wave dispersion is well captured in our simulation and the overall agreement is very good. Wave runup for case  $d=61$  mm is 5.4 mm, comparing to 6.2 mm in the experiment, and for case  $d=120$  mm, the wave runup is 2.3 mm, comparing to 3.4 mm in the experiment.

## 4.2 Benchmark Problem #4 - Two-dimensional submarine granular slide

The computational domain used in TSUNAMI3D for the submarine glass bead landslide (test 17) is constructed using exactly the same experiment dimensions of benchmark problem #4. Cell sizes for the numerical simulation are  $\sim 5$  mm in both  $x$  and  $y$  directions and  $\sim 1$  mm in  $z$ . This results in 18.8 million computational cells. The time step  $\Delta t$  ranges from 0.000125 s to 0.00125 s. Reflection boundary conditions are applied to all walls except for the runup side. Slide density is set to  $1950 \text{ kg/m}^3$ .

We achieved the best results considering Newtonian fluid for the landslide

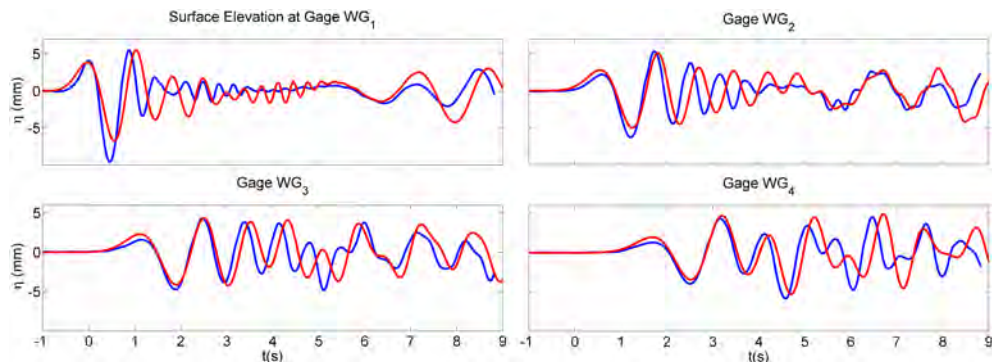


Figure 3: Comparison of gauge time series between TSUNAMI3D (red) and 3D solid block landslide experiment (blue) (test 17).

material with a water eddy viscosity of  $1 \times 10^{-5} \text{ m}^2/\text{s}$  and slide eddy viscosity of  $1 \times 10^{-4} \text{ m}^2/\text{s}$ . We also tested the slide material using the simplified rheology (Eq. 6) to bring the slide to a stop, but observed very little difference on the ensuing waves.

In general, TSUNAMI3D achieved relatively good results, especially for the two leading waves. From Fig. 3, it can be observed that our model underpredicts the trough by a small amount, and the trailing waves are moving slower, but the overall pattern match very well with the experiment. This can be attributed, possibly, to the slightly dispersion of the granular material which is not considered in the model (no change of volume)

### 4.3 Benchmark Problem #7 - Field Case: Slide at Port Valdez, AK during 1964 Alaska Earthquake

We used the model TSUNAMI3D to simulate the HPV slide (landslide at the head of Port Valdez) and the SBM slide (landslide at the Shoup Bay moraine) separately. The computational grid was converted from spherical coordinates (longitude/latitude) to Cartesian ( $x/y$ ) coordinates. In both simulations, cell sizes in both  $x$  and  $y$  directions are approximately 13 m, while in the vertical direction  $z$ , the cell size is variable, starting from 1.0 m at the still water level and increasing gradually to  $\sim 2.0$  m toward the bottom, while being kept constant at 1.0 m on top of the still water level. This results in 343.4 million computational cells. The time step  $\Delta t$  is also variable, from 0.01 s to 0.1 s. An outflow boundary condition is applied to the south boundary, and



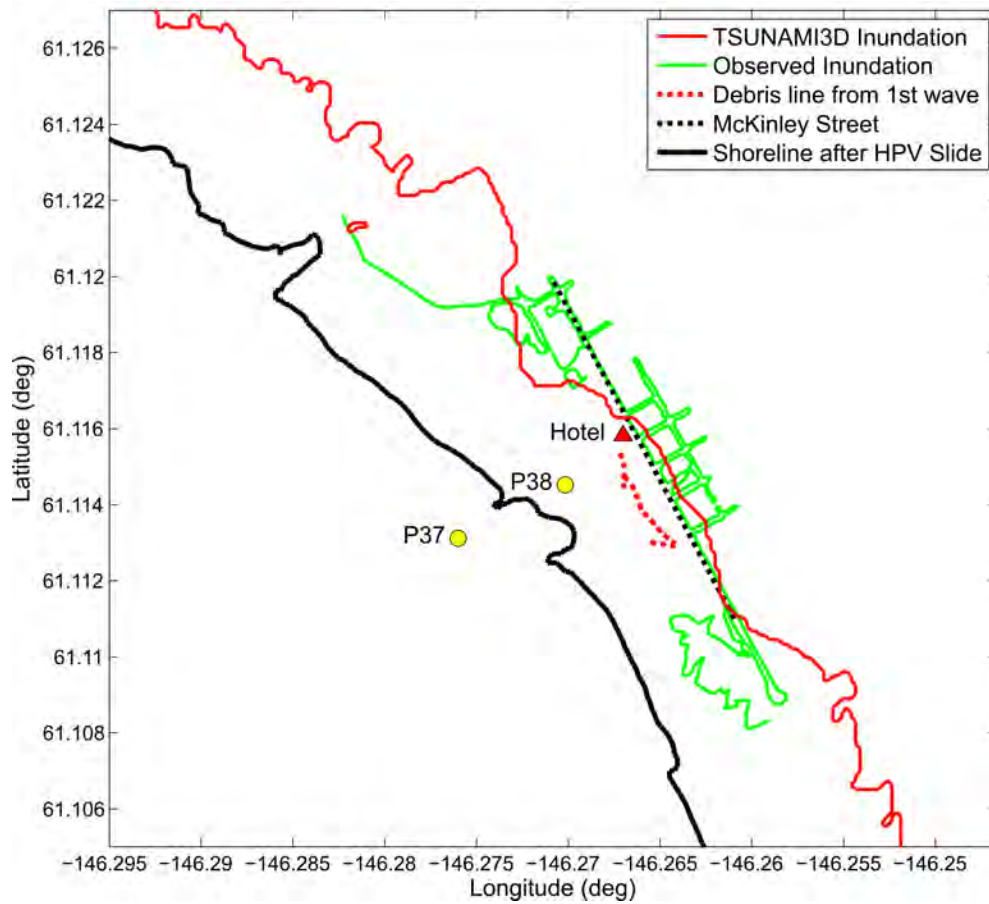


Figure 4: Comparison between observation data and TSUNAMI3D results. Red solid line represents the inundation line from TSUNAMI3D simulation. Green solid lines represent the the observed inundation line. Red dashed line marks the debris from the first wave, and the black dashed line marks the McKinley Street. The Valdez Hotel is denoted by a red triangle. The post-earthquake shoreline is shown in solid black line.

a no-slip condition is applied to the bottom. In addition, a first order finite difference scheme is used for the nonlinear terms in the momentum equations for this problem.

Fig. 4 shows a comparison between the tsunami observation data and TSUNAMI3D results. The red solid line represents the inundation limit from the numerical simulation. We find good agreement with the observed

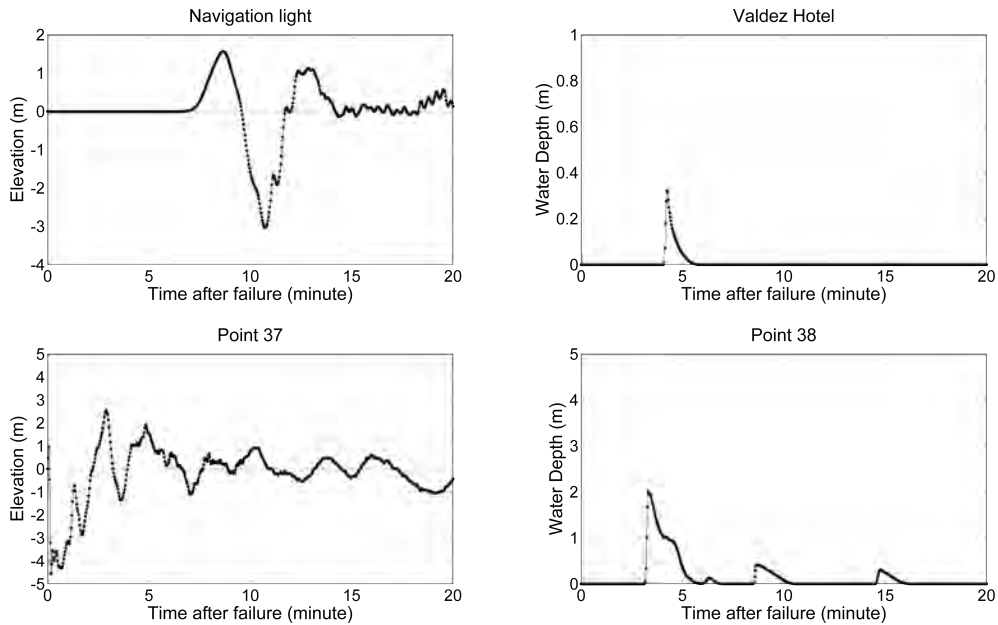


Figure 5: TSUNAMI3D HPV landslide simulation surface elevation time series at four gauge locations. The navigation light is at Valdez Narrows and the Valdez Hotel is the red triangle in Fig. 4. Point 37 and 38 are the gauge locations digitized from Figure 23 in [Nicolisky et al., 2013], which are shown in Fig. 4.

inundation limit (green solid line). The inundation reaches the McKinley Street (black dashed line), and floods the Valdez Hotel. Fig. 5 shows the surface elevation time series at four gauge locations. Gauge 37 shows a -4.5 m withdrawal within 1 minute following the landslide and then a 2.5 m wave amplitude around 3 minutes, and a second wave of about 2.0 m around 5 minutes. Likewise, gauge 38 recorded a 2.0 m maximum water depth shortly after 3 minutes, followed by two smaller inundation fronts. At the Valdez Hotel, a 0.3 m inundation is recorded around 4 minutes. The navigation light recorded two major waves of 4.6 m and 4.1 m wave height (crest to trough).

Fig. 6 is a contour plot of the maximum wave and runup height of TSUNAMI3D SBM landslide tsunami. The SBM landslide tsunami inundated the Valdez port. The maximum runup at Anderson bay is 25 m, while the maximum runup at Cliff Mine (closer to the source) is 30 m. In Fig. 7, three major short waves of  $\sim 1$  minute period hit the navigation light, with

maximum wave amplitude of 8.3 m.

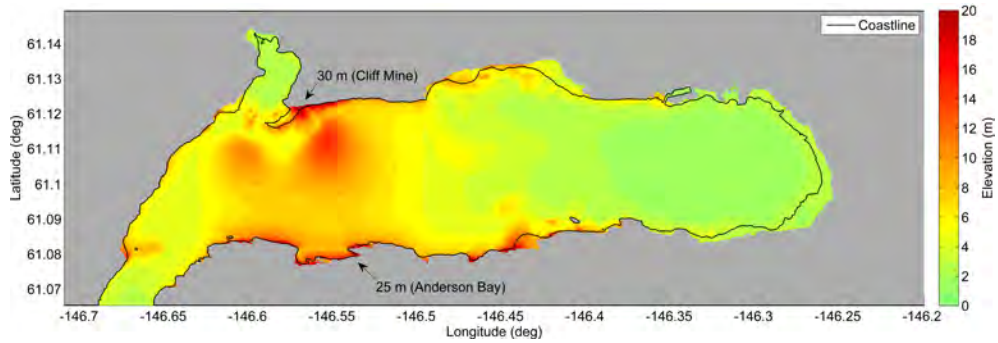


Figure 6: Maximum wave and runup height contour plot of TSUNAMI3D SBM landslide tsunami. The black line is the coastline.

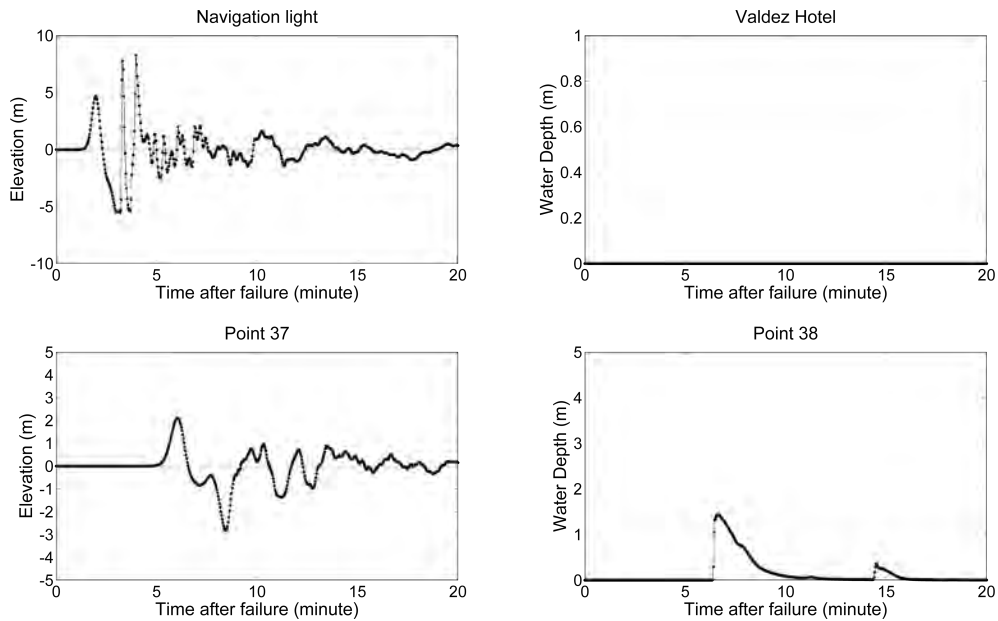


Figure 7: TSUNAMI3D SBM landslide simulation surface elevation time series at four gauge locations. The navigation light is at Valdez Narrows and the Valdez Hotel is the red triangle in Fig. 4. Point 37 and 38 are the gauge locations digitized from Figure 23 in [Nicolosky et al., 2013], which are shown in Fig. 4.

## 5 Conclusions

Overall, we find quite good agreement between the data and TSUNAMI3D's model results in all benchmark problems. For the two laboratory experiments, benchmark problem #2 and #4, we achieved very good agreement in wave period and magnitude, especially for the leading waves. However, we also found that the trailing waves are moving slower than the ones recorded in the experiments.

In benchmark problem #7, the landslide at the head of Port Valdez (HPV) generated an inundation line along the McKinley Street, matching the field observation quite well. Numerical gauges at point 37 and 38 recorded at least two major waves and the Valdez Hotel gauge recorded a 0.3 m water depth. The slide at the Shoup Bay moraine generated a 25m runup near the Anderson Bay, and an 8.3 m wave hitting the navigation light, matching observations relatively well.

## 6 Acknowledgments

The authors are grateful for the valuable help from Dr. Jim Kirby (University of Delaware) and Dr. Stephan Grilli (University of Rhode Island) in organizing the workshop. We also are grateful for the unconditional help of TAMU Ocean Engineering department head, Dr. Sharath Girimaji, for accomodating and providing transportation for the workshop participants. The authors also wish to thank the NTHMP and the National Oceanic and Atmospheric Administration (NOAA) for providing funding for the activities associated with this workshop at the Texas A&M University at Galveston.

## References

- [Forterre and Pouliquen, 2008] Forterre, Y. and Pouliquen, O. (2008). Flows of dense granular media. *Annu. Rev. Fluid Mech.*, 40:1–24.
- [Heinrich and Piatanesi, 2000] Heinrich, P. and Piatanesi, A. (2000). Near-field modeling of the july 17,1998 tsunami in papua new guinea. *Geophysical Research Letters*, 27:3037–3040.

- [Hirt and Nichols, 1981] Hirt, C. W. and Nichols, B. D. (1981). Volume of fluid (VOF) method for the dynamics of free boundaries. *Journal of Computational Physics*, 39:201–225.
- [Horrillo et al., 2013] Horrillo, J., Wood, A., Kim, G.-B., and Parambath, A. (2013). A simplified 3-d navier-stokes numerical model for landslide-tsunami: Application to the Gulf of Mexico. *J. Geophys. Res. Oceans*, 118:6934–6950.
- [Horrillo, 2006] Horrillo, J. J. (2006). *Numerical methods for tsunami calculation using full Navier-Stokes equations and the volume of Fluid method*. PhD thesis, University of Alaska, Fairbanks, Alaska.
- [Nicolosky et al., 2013] Nicolosky, D. J., Haeussler, E., Ryan, P., Koehler, H., Combellick, R., and Hansen, R. (2013). Tsunami inundation maps of port valdez, alaska.